

STUDY OF EXCITONIC TRANSITIONS IN δ -DOPED GaAs/AlAs QUANTUM WELLS

B. Čechavičius^a, R. Nedzinskas^a, J. Kavaliauskas^a, V. Karpus^a, G. Valušis^a,
B. Sherliker^b, M. Halsall^b, P. Harrison^c, E. Linfield^c, and M. Steer^d

^a *Semiconductor Physics Institute, A. Goštauto 11, LT-01108 Vilnius, Lithuania*

E-mail: bronius@pfi.lt

^b *School of Electronic and Electrical Engineering, University of Manchester, Manchester M60 1QD, United Kingdom*

^c *IMP, School of Electronic and Electrical Engineering, University of Leeds, Leeds LS2 9JT, United Kingdom*

^d *Department of Electronic and Electrical Engineering, University of Sheffield, Mappin St, Sheffield S1 3JD, United Kingdom*

Received 11 June 2009; revised 9 September 2009; accepted 15 September 2009

Investigation of excitonic lines in differential surface photovoltage (DSPV) spectra of *p*-type (Be) δ -doped GaAs/AlAs multiple quantum well (MQW) structures is reported. From the lineshape analysis of the DSPV spectra, the energies and line broadening parameters for a large number of QW related excitonic transitions were determined. It is found that transition energies are in a good agreement with calculations carried out within the envelope function approximation taking into account the nonparabolicity of energy bands. Examining the dependence of the exciton linewidth on the QW thickness, the line-broadening mechanisms were revealed and interface roughness in the MQW structures was evaluated. An asymmetrical lineshape of certain excitonic transitions in SPV spectra of MQW structures was shown to be related to the Fano resonance.

Keywords: delta-doped quantum wells, surface photovoltage spectroscopy, excitonic transitions

PACS: 73.21.Fg, 78.55.Cr, 78.67.De

1. Introduction

The strong interest in δ -doped quantum wells (QWs) is motivated by the potential application of the nanostructures as active media in compact terahertz (THz) devices ([1] and references herein). The tunability of the energy levels of shallow impurities embedded in QWs opens up the possibility to vary the THz detection frequency by changing the profile of QW confining potential [2, 3]. It is expected that this particular material system with Be dopants in GaAs/AlAs heterostructures will provide detectors covering the wavelength range from 40 to 60 μm (7.5–5 THz). In GaAs, beryllium is an acceptor impurity-doped species commonly used in devices, and it is relatively stable with respect to diffusion. To find an optimal device design, it is of particular importance to know an electronic structure and physical properties of the QW structures, such as presence of imperfections, interface quality, and internal electric fields. The information needed can be obtained by modulation spectroscopy methods, which allow one to study QW structures with high spectral sensitivity. During the last years, we have employed the contact-

less methods of photoreflectance and differential surface photovoltage (DSPV) for the characterization of Be δ -doped GaAs/AlAs MQW structures designed for THz sensing applications [4–6]. So far the investigations have been mainly performed at room temperature. In this work, to gain further insight into the excitonic properties with increasing doping level, we extended our previous DSPV spectroscopy studies [4, 6] of Be δ -doped GaAs/AlAs multiple QW (MQW) structures to low temperature region of 90 K. The lineshape analysis of the DSPV spectra allowed us to extract information on the excitonic parameters for a large number of QW subbands. Special attention was paid to an exciton line broadening mechanism in MQWs. A high quality of the studied samples allows us to observe the Fano resonance effect [7] for definite excitonic lines in the SPV spectrum.

2. Samples and experiment

A series of Be δ -doped GaAs/AlAs MQWs were grown by MBE on a semi-insulating (100) GaAs

Table 1. Characteristics of the samples: the repeated period, the quantum well width L_w , the δ -doping Be concentration N_A , and the growth temperature of the epitaxial layer T . N_D signifies the δ -doping Si concentration.

Samples	Periods	L_w (nm)	N_A (cm ⁻²)	T (°C)
1795	400	3	$2 \cdot 10^{10}$	550
2068	300	5	$5 \cdot 10^{10}$	550
1794	200	10	$5 \cdot 10^{10}$	550
1303	50	15	$2.5 \cdot 10^{12}$	540
1392	40	20	$2.5 \cdot 10^{12}$	540
1807	100	20	$5 \cdot 10^{10}$	550
L80	40	15	undoped	700
L29	40	20	Si: $N_D = 4 \cdot 10^9$	670

substrate. Prior to the growth of the MQWs, a 300 nm thick GaAs buffer layer was grown. Each of the MQW structures investigated contained the same, 5 nm wide AlAs barrier, while each GaAs well layer was δ -doped at the well centre with Be acceptors. The structures were capped with a 100 nm GaAs layer. For comparison, undoped and weakly Si δ -doped MQWs were also studied. The doping level and the main characteristics of samples are summarized in Table 1. The SPV measurements were done in a chopped light geometry using a capacitor-like system with a transparent conducting top electrode under normalized incident light intensity conditions [8]. The illumination intensity was selected at sufficiently low levels in order not to affect the line shape of the spectra. In DSPV spectra measurements, a wavelength-modulation technique was used. The wavelength of the incident probe light was modulated by vibrating a fused-silica plate at 87 Hz located near the exit slit of the monochromator. The SPV and wavelength-modulated DSPV signals were recorded by a conventional lock-in detection system. The measurements were performed at 90 K temperature.

3. Experimental results and discussion

3.1. DSPV spectra

Figure 1 shows the typical DSPV spectra for the Be δ -doped GaAs/AlAs MQW structures (Table 1). At energies higher than band gap E_g of GaAs (1.506 eV at 90 K), the spectra are dominated by the optical features $mnH(L)$ which correspond to excitonic transitions in the MQW region of the samples. The notation $mnH(L)$ signifies the transitions between the m th electron and n th heavy-hole (H) or light-hole (L) subbands. By considering excitonic features we assumed that the spectra of the normalized DSPV/SPV signal are qualitatively equivalent to the first derivative of the absorption spec-

tra. The energies and broadening parameters of the optical transitions responsible for the observed DSPV features were determined by best fits of the DSPV spectra to the first derivative of a Lorentzian-type function [9]. As can be seen from Fig. 1, the experimental DSPV data (open circles) are reasonably well described by the adopted lineshape model (full lines). The optical transition energies (arrows in Fig. 1) were found to vary with the QW thickness L_w as expected from the quantum confinement effect. The heavy- and light-hole related excitonic transitions are well resolved due to comparatively small broadening of the energy states at 90 K. Also, it was observed that the shift of excitonic features of ~ 82 meV with respect to their positions at room temperature [4] is in good agreement with the temperature shift of the GaAs bandgap energy.

3.2. Optical transition energies

To identify the optical features observed, we have carried out calculations of energy levels and interband transition energies for GaAs/AlAs QWs studied. The transition energies were primarily calculated for undoped rectangular QW both for parabolic and nonparabolic energy bands in the envelope function approximation [10]. We used the parameters of calculations employed in our previous work [4]. The calculations of energy levels by solving Poisson and Schrödinger equations have also been performed in order to study possible effects arising from the δ -doping. It was found that the change in the ground state optical transition energy due to a distortion of the rectangular QW potential profile by δ -doping is negligible and reaches only ≤ 3 meV for the acceptor density of $2.5 \cdot 10^{12}$ cm⁻² in the 20 nm QW. For the narrower QWs and higher order optical transitions the deviations were found to be even smaller. It is worth noting that a solution of the coupled Poisson-Schrödinger equations has shown that the QWs with the acceptor density of $2.5 \cdot 10^{12}$ cm⁻² should not be degenerate.

The results of the calculation and experimental data are presented in Fig. 2. Symbols represent the experimental excitonic energies determined from the fitting procedure, while the lines correspond to theoretical results, obtained within the nonparabolic energy bands' approximation. It should be noted that the calculated transition energies slightly differ from experimental ones for GaAs/AlAs MQW sample with $L_w = 3$ nm (Fig. 2). The well width L_w of the narrow QWs can be slightly different from a nominal value due to a possible technological inaccuracy. However, generally, the experimental data are in quite good agreement

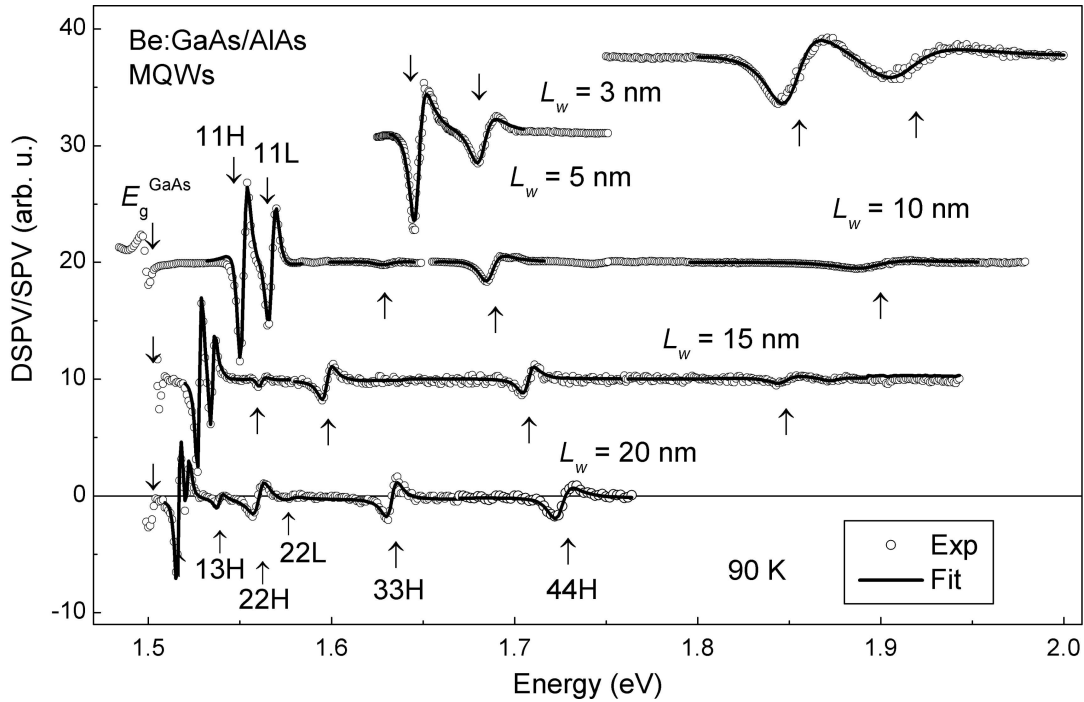


Fig. 1. DSPV spectra of Be δ -doped GaAs/AlAs MQWs for different well width L_w measured at 90 K. The arrows show the excitonic transitions energies obtained from a best fit of experimental data (open circles) to the first derivative of a Lorentzian-type function (solid curves).

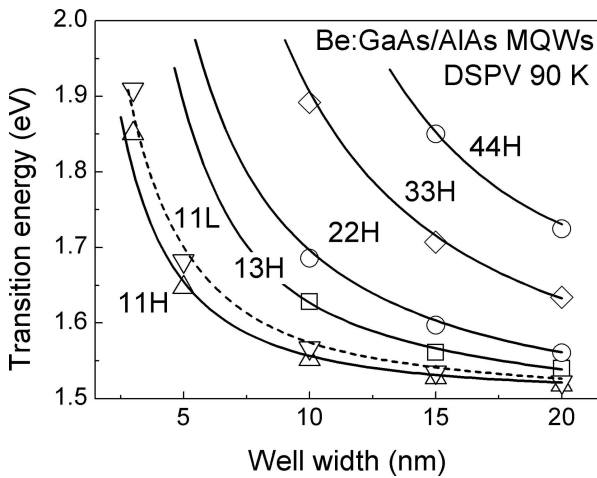


Fig. 2. The experimental (symbols) and calculated (lines) dependences of interband transition energies on QW width L_w for Be δ -doped GaAs/AlAs MQWs. The results of calculations are presented for nonparabolic energy bands' approximation.

with calculations. It was found that for most optical transitions studied the calculated interband energies exceed the experimental data by ~ 5 – 10 meV. The difference should be equal to exciton binding energy that was not included in our calculations. However, it is somewhat smaller than the exciton binding energies in the undoped GaAs/AlAs QWs obtained from photoluminescence excitation studies [11]. It seems likely that the differences could be attributed to many-body effects

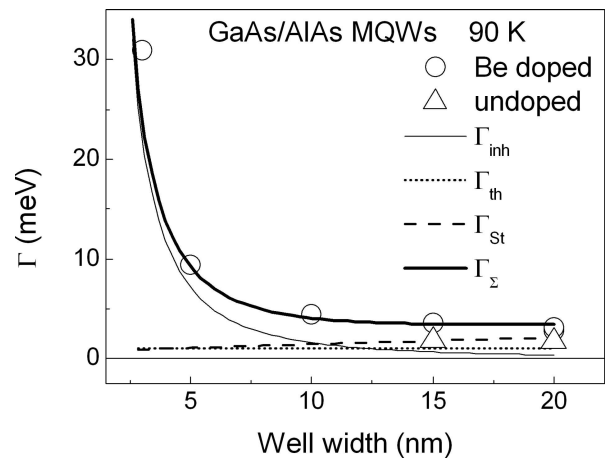


Fig. 3. Experimental (open circles) and calculated (thick solid curve) linewidth Γ of 11H excitonic transitions in Be δ -doped GaAs/AlAs MQWs as a function of the well width L_w . The calculated contributions to the line broadening due to well width fluctuations Γ_{inh} (thin solid curve), exciton interaction with phonons Γ_{th} (dotted line), and broadening induced by random electric fields of ionized impurities Γ_{St} (dashed curve) are also presented. In addition, broadening parameters of undoped and weakly Si-doped MQWs are shown for comparison (triangles).

[12]. However, the details of exciton binding energies is not the subject of the present work.

3.3. Broadening mechanisms of the spectral lines

The DSPV spectra of Be δ -doped GaAs/AlAs MQWs (Fig. 1) exhibit a well-resolved 11H feature associated with ground state QW excitonic transitions. The well-resolved optical feature allows to extract information about excitonic line broadening mechanisms and interfacial properties, which define the quality of the structures studied. The well width dependence of the broadening parameter Γ , which represents the full width at half maximum (FWHM) of the lowest energy exciton line, is presented by open circles in Fig. 3. In addition, experimental values of the broadening parameter for undoped and weakly Si-doped MQW samples are presented for comparison (open triangles). As can be seen, the linewidth for Be-doped samples decreases with the QW width from 31 to about 3 meV. However, the lowest Γ value in Be-doped samples remains to be somewhat larger than Γ in undoped and weakly Si-doped samples (~ 2 meV).

By analysing the experimental $\Gamma(L_w)$ dependences, several line broadening mechanisms were considered [13]: (i) thermal broadening (Γ_{th}) due to phonon scattering, (ii) inhomogeneous broadening of the exciton energy levels (Γ_{inh}) caused by structural imperfections, first at all by interface roughness in the QWs, and (iii) broadening due to the Stark effect in a random Coulomb field of ionized impurities (Γ_{St}).

Considering the thermal broadening contribution, we used the value of $\Gamma_{th} = 1$ meV (Fig. 3, dotted line) estimated from the temperature dependence of exciton scattering by phonons in GaAs/AlGaAs QWs [14].

The inhomogeneous line broadening Γ_{inh} due to the well width fluctuations was evaluated as the change of the exciton energy E_n with the variation of the well width [15], i. e. $\Gamma_{inh} = 2.36(dE_n/dL_w)\delta L_w$, where δL_w is the standard deviation of the well width fluctuations obeying a Gaussian distribution and n is the quantum number of the QW subbands. The δL_w in thick QWs, where 11H optical transitions are insensitive to a variation in L_w (Fig. 2), were evaluated from the broadening of the higher order quantum confined transitions by examining experimental $\Gamma(n)$ dependences (see [4] for details). The well width fluctuations δL_w were found to be equal to ~ 0.6 , ~ 0.8 , and ~ 1.0 monolayer (1 ML = 2.83 Å) in samples L29, 1392, and 1807, respectively. It should be noted that for $\delta L_w = 1$ ML, inhomogeneous broadening parameter Γ_{inh} is 0.8 meV and 50 meV for the 20 and 3 nm QW widths, respectively. Thus, whereas Γ_{inh} is smaller than the observed linewidth for the widest, 20 nm, QW, it is much larger

than the linewidth for the narrowest, 3 nm, QW. The latter result indicates that actually δL_w in narrower QWs must be smaller than 1 ML.

The well width fluctuations in narrow QWs were estimated by analysing the total $\Gamma(L_w)$ dependence as the sum $\Gamma = \Gamma_{th} + \Gamma_{inh} + \Gamma_{St}$ of partial contributions. To perform such analysis, the Stark broadening Γ_{St} in a random Coulomb field of ionized impurities was estimated by the relation $\Gamma_{St} = 2 \cdot 10^{-30} N_i^{4/3} (m_0/\mu)^2 E_b^{-1}$ derived for the bulk, 3D, case in [16], where N_i is the concentration of ionized impurities, E_b is the exciton binding energy, m_0 is the free electron mass, and μ is the reduced electron-heavy hole mass. The experimental data for the Be-doped QWs (Fig. 3, open circles) were fitted reasonably by choosing $\delta L_w = 0.5$ ML (Fig. 3, thin solid curve representing Γ_{inh}) and $N_i = 8 \cdot 10^{16} \text{ cm}^{-3}$ (Fig. 3, dashed curve representing Γ_{St}). One may suppose that the smaller δL_w values estimated in narrow QWs as compared to the thick ones could be due to the correlation effects of well width fluctuations in narrow QWs [17]. Note also, that concentration of ionized impurities $N_i = 8 \cdot 10^{16} \text{ cm}^{-3}$, deduced from the Γ -analysis, corresponds to a density $N_i \sim 1.6 \cdot 10^{10} \text{ cm}^{-2}$ in the weakly doped samples at 90 K. It should be noted as well that, contrary to the room temperature results [4, 6], the broadening parameter Γ only slightly depends on doping level at 90 K (see data in Fig. 3 of $L_w = 15$ and 20 nm, which correspond to 1807 and 1392 samples). To explain this effect, one can propose that Coulomb potential of the charged acceptors, located within the plane of δ -layer, is screened at low temperature by free holes [18], and the exciton broadening by ionized impurities is suppressed.

3.4. Influence of Fano coupling on excitonic transitions

The remainder part is devoted to the study of the lineshape features of higher order excitonic transitions that are degenerate with the continuum of the excitonic states related with lower subband pairs. In this case the spectral changes of both the discrete lines and continuum can be expected due to Fano resonance effect [7]. For example, Fano resonance was predicted [19] for the weakly allowed 13H transition, but in comparison with experiment it was hampered by a large inhomogeneous broadening Γ_{inh} introduced by fabrication process of the samples. We believe that a small Γ_{inh} value revealed for the our widest 20 nm QW should allow us to observe the Fano resonance spectroscopically.

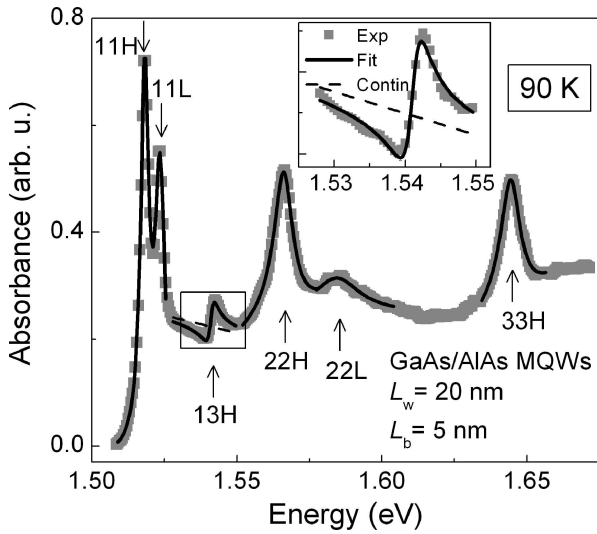


Fig. 4. Absorption spectrum of Be δ -doped GaAs/AlAs MQWs with well width $L_w = 20$ nm (sample 1807, Table 1) at 90 K. The arrows show the transition energies obtained from a best fit of experimental data (open squares) to Eq. (1) (solid curves). The inset shows an expanded view of the Fano resonance associated 13H transition.

Figure 4 shows the absorbance spectrum for the Be-doped GaAs/AlAs MQW structure with 20 nm QW (Table 1, 1807 sample), calculated from normalized SPV measurements. From an analysis of the spectrum it follows that the two lowest 11H and 11L peaks, corresponding to heavy- and light-hole ground state excitonic transitions, manifest a Lorentzian-like lineshapes. In contrast, the higher order excitonic transitions 13H, 22H, and 33H exhibit asymmetric lineshapes and can be interpreted as Fano resonances arising from an interaction of these discrete excitonic states with the continua of lower lying energy levels. The Fano line shape, with a dip below the continuum absorption on the low-energy side, is most distinctly pronounced for the 13H exciton.

To characterize the spectral asymmetry of the 13H, 22H, and 33H lines (Fig. 4), we have fitted the observed optical features to the phenomenological Fano line-shape function [7]

$$\alpha = \alpha_{\text{cont}} \frac{(q + \varepsilon)^2}{1 + \varepsilon^2}, \quad (1)$$

where q is the ratio between the optical matrix elements of transitions to the discrete state and to the continuum, ε is normalized energy defined by $\varepsilon = 2(E - \Omega)/\Gamma$, Ω is the energy of the corresponding Fano resonance, Γ is the broadening (linewidth) of resonant state due to the Fano coupling, and α_{cont} describes the absorption of the continuum without coupling. Depending on the sign of q , which itself depends on the relative signs of

the transition and coupling matrix elements, Eq. (1) describes a line shape with the dip on the low ($q > 0$) or high ($q < 0$) energy side of the peak. A fitting of the experimental data (squares) to the Fano function (1) is presented by curves in Fig. 4. The fitting shows that the 22H and 33H lines are almost symmetric ($q = -12$) and practically do not present a Fano resonance, while the 13H line (see inset of Fig. 4) presents a very distinct Fano resonance ($q = 1.3$) indicating a strong coupling. This could be associated with a relatively weak oscillator strength of the forbidden 13H transitions. Note also that q is positive, i. e., the dip occurs below the exciton peak. The lineshape is in agreement with theoretical calculation [19] and experimental observations in other QWs [20].

4. Conclusions

In summary, DSPV spectra of Be δ -doped GaAs/AlAs MQW structures have been measured at 90 K temperature. From the lineshape analysis of DSPV spectra the transition energies and line-broadening parameters for a large number of QW-related excitonic transitions were determined. The transition energies were found to be in a good agreement with the calculated ones for non-parabolic energy bands. It was revealed that in QWs thinner than 10 nm the dominant line broadening mechanism is due to the half-ML well-width fluctuations. In QWs thicker than 10 nm, the average well width fluctuations are found to be 0.6–1 ML. In thick QWs, the thermal broadening, the inhomogeneous line broadening due to well width fluctuations, and Stark broadening due to the random electric fields of the ionized impurities contribute to the observed line broadening Γ . In addition, the distinct behaviour of the Fano resonance of forbidden 13H excitonic transitions in SPV spectra for 20 nm wide QWs was disclosed.

Acknowledgements

The work was supported, in part, by the Lithuanian State Science and Studies Foundation under contract C-07004/C-17/2009 project.

The research in the Semiconductor Physics Institute is conducted under topics *Optical spectroscopy of composite nanostructures and quantum structures (158J)* and *Terahertz optoelectronics: Devices and applications (179J)*.

References

- [1] D. Seliuta, B. Čechavičius, J. Kavaliauskas, S. Balauskas, G. Valušis, B. Sherliker, M.P. Halsall, P. Harrison, M. Lachab, S.P. Khanna, and E.H. Linfield, Impurity bound-to-unbound terahertz sensors based on beryllium and silicon δ -doped GaAs/AlAs quantum wells, *Appl. Phys. Lett.* **92**, 053503-1–3 (2008).
- [2] W.M. Zheng, M.P. Halsall, P. Harmer, P. Harrison, and M.J. Steer, Acceptor binding energy in δ -doped GaAs/AlAs multiple-quantum wells, *J. Appl. Phys.* **92**, 6039–6042 (2002).
- [3] W.M. Zheng, M.P. Halsall, P. Harrison, J.-P.R. Wells, I.V. Bradley, and M.J. Steer, Effect of quantum-well confinement on acceptor state lifetime in δ -doped GaAs/AlAs multiple quantum wells, *Appl. Phys. Lett.* **83**, 3719–3722 (2003).
- [4] B. Čechavičius, J. Kavaliauskas, G. Krivaitė, D. Seliuta, G. Valušis, M.P. Halsall, M.J. Steer, and P. Harrison, Photorefectance and surface photovoltage spectroscopy of beryllium-doped GaAs/AlAs multiple quantum wells, *J. Appl. Phys.* **98**, 023508-1–8 (2005).
- [5] B. Čechavičius, J. Kavaliauskas, G. Krivaitė, D. Seliuta, E. Širmulis, J. Devenson, G. Valušis, M.P. Halsall, M.J. Steer, and P. Harrison, Optical and terahertz characterization of Be-doped GaAs/AlAs multiple quantum wells, *Acta Phys. Pol. A* **107**, 328–332 (2005).
- [6] B. Čechavičius, J. Kavaliauskas, G. Krivaitė, V. Karpus, D. Seliuta, G. Valušis, M.P. Halsall, M.J. Steer, and P. Harrison, Study of Be δ -doped GaAs/AlAs multiple quantum wells by surface photovoltage spectroscopy, *Appl. Surf. Sci.* **252**, 5437–5440 (2006).
- [7] U. Fano, Effects of configuration interaction on intensities and phase shifts, *Phys. Rev.* **124**, 1866–1878 (1961).
- [8] S. Datta, S. Ghosh, and B.M. Arora, Electoreflectance and surface photovoltage spectroscopy of semiconductor structures using an indium-tin-oxide-coated glass electrode in soft contact mode, *Rev. Sci. Instrum.* **72**, 177–183 (2001).
- [9] D.E. Aspnes, Third-derivative modulation spectroscopy with low-field electoreflectance, *Surf. Sci.* **37**, 418–442 (1973).
- [10] V. Karpus, *Two-dimensional Electrons* (Ciklonas, Vilnius, 2004) [in Lithuanian].
- [11] M. Gurioli, J. Martinez-Pastor, M. Colocci, A. Bosacchi, S. Franchi, and L.C. Andreani, Well-width and aluminium concentration dependence of the exciton binding energies in GaAs/Al_xGa_{1-x}As quantum wells, *Phys. Rev. B* **47**, 15755–15762 (1993).
- [12] J.P. Loehr and J. Singh, Nonvariational numerical calculations of exciton properties in quantum wells in the presence of strain, electric fields, and free carriers, *Phys. Rev. B* **42**, 7154–7162 (1990).
- [13] P.J. Stevens, M. Whitehead, G. Parry, and K. Woodbridge, Computer modeling of the electric field dependent absorption spectrum of multiple quantum well material, *IEEE J. Quantum Electron.* **24**, 2007–2016 (1988).
- [14] A. Venu Gopal, Rajesh Kumar, A.S. Vengurlekar, A. Bosacchi, S. Franchi, and L.N. Pfeiffer, Photoluminescence study of exciton–optical phonon scattering in bulk GaAs and GaAs quantum wells, *J. Appl. Phys.* **87**, 1858–1862 (2000).
- [15] K.K. Bajaj, Use of excitons in materials characterization of semiconductor system, *Mater. Sci. Eng. R Rep.* **34**, 59–120 (2001).
- [16] N. Dai, F. Brown, R.E. Doezema, S.J. Chung, and M.B. Santos, Temperature dependence of exciton linewidths in InSb quantum wells, *Phys. Rev. B* **63**, 115321-1–6 (2001).
- [17] I.V. Ponomarev, L.I. Deych, and A.A. Lisyanski, Interface disorder and inhomogeneous broadening of quantum well excitons: Do narrow lines always imply high-quality interfaces? *Appl. Phys. Lett.* **85**, 2496–2499 (2004).
- [18] R.N. Riemann, C. Metzner, and G.H. Döhler, Density-dependent intersubband absorption in strongly disordered systems, *Phys. Rev. B* **65**, 115304-1–10 (2002).
- [19] H. Chu and Y.-C. Chang, Theory of line shapes of exciton resonances in semiconductor superlattices, *Phys. Rev. B* **39**, 10861–10871 (1989).
- [20] D.Y. Oberli, G. Böhm, G. Weimann, and J.A. Brum, Fano resonances in the excitation spectra of semiconductors quantum wells, *Phys. Rev. B* **49**, 5757–5760 (1994).

EKSITONINIŲ ŠUOLIŲ GaAs/AlAs KVANTINĖSE DUOBĖSE SU PRIEMAIŠOMIS TYRIMAS

B. Čechavičius^a, R. Nedzinskas^a, J. Kavaliauskas^a, V. Karpus^a, G. Valušis^a, B. Sherliker^b, M. Halsall^b,
P. Harrison^c, E. Linfield^c, M. Steer^d

^a Pūslaidininkų fizikos institutas, Vilnius, Lietuva

^b Mančesterio universitetas, Mančesteris, Jungtinė Karalystė

^c Lydso universitetas, Lydsas, Jungtinė Karalystė

^d Šefildo universitetas, Šefildas, Jungtinė Karalystė

Santrauka

Plėtojant THz prietaisų technologiją, svarbu detaliam žinoti kvantinių duobių su priemaišomis energinę sandarą ir optines savybes. Šiame darbe diferencialinio paviršinio fotovoltinio atsako metodu ištirti GaAs/AlAs kvantinių duobių su berilio priemaišomis eksitoninių optinių šuolių ypatumai. Bandinius sudarė skirtingo pločio L_w GaAs duobių su 5 nm storio AlAs barjeriais dariniai. Duobių centrinėje srityje buvo įterptas Be akseptorių sluoksnis. Priemaišų tankis kito nuo $5 \cdot 10^{10}$ iki $2,5 \cdot 10^{12} \text{ cm}^{-2}$. Tyrimų rezultatai rodo, jog optinį bandinių atsaką lemia eksitoniniai šuoliai, o sugerties linijos formą veikia Fano efektas. Optinių šuolių prigim-

tis buvo atskleista apskaičiavus energijos lygmenis pernašos matricų metodu. Eksperimentinės optinių šuolių energijos vertės dera su teorinėmis, apskaičiuotomis atsižvelgiant į energijos juostų neparaboliškumą. Išanalizavus eksitoninių linijų išplitimo parametrų priklausomybes nuo duobės pločio bei priemaišų tankio, buvo nustatyti eksitoninių linijų išplitimo mechanizmai. Gauti rezultatai rodo, kad tirtose kvantinėse duobėse pasireiškia keletas linijos išplitimo veiksnių. Siaurose duobėse ($\leq 5 \text{ nm}$) linijos išplitimą lemia kvantinių duobių pločio fliktuacijos ($\delta L_w \leq 0,5$ sluoksnio); platesnėse duobėse eksitonų linija išplinta visų pirma dėl sąveikos su fononais ir jonizuotomis priemaišomis.